

Density Functional Theory Study on the Aggregation and Dissociation Behavior of Lithium Chloride in THF and Its Interaction with the Active Centers of the Anionic Polymerization of Methyl Methacrylate and Styrene

Alexander V. Yakimansky,^{†,‡} Axel H. E. Müller,^{*,†,§} and Marcel Van Beylen^{*,||}

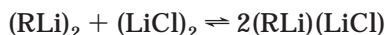
Institut für Physikalische Chemie, Johannes Gutenberg Universität, Welderweg 15, D-55099 Mainz, Germany; and Laboratory of Macromolecular and Physical Organic Chemistry, Katholieke Universiteit Leuven, Celestijnenlaan 200 F, B-3001 Heverlee, Belgium

Received December 27, 1999; Revised Manuscript Received April 10, 2000

ABSTRACT: The structure of LiCl in tetrahydrofuran (THF) solution and its effect on the structure and stability of active sites of the anionic polymerization of methyl methacrylate (MMA) and styrene (St) was studied using the quantum-chemical density functional theory (DFT) approach. In the case of MMA anionic polymerization, it was found that LiCl forms stable mixed aggregates with ester enolates that model the PMMA living chain ends, thus preventing them from self-aggregation. They may even stabilize more reactive zwitterionic structures of these chain ends. The dissociation of solvated LiCl dimers to form $\text{Li}^+(\text{THF})_4$ cations is slightly endothermic in THF, while scavenging of $\text{Li}^+(\text{THF})_4$ by LiCl dimers to produce more stable quintuple cations $[(\text{THF})_3\text{Li}-\text{Cl}-\text{Li}(\text{THF})_2-\text{Cl}-\text{Li}(\text{THF})_3]^+$ is even exothermic. Therefore, if the concentration of LiCl exceeds a certain threshold value, $\text{Li}^+(\text{THF})_4$ cations should effectively be scavenged by LiCl dimers. Thus, increasing LiCl concentration below the threshold concentration should lead to an increase in the concentration of free $\text{Li}^+(\text{THF})_4$ cations. In the anionic polymerization of styrene in the presence of LiCl this results in the suppression of $\text{PSt}-\text{Li}$ chain end dissociation due to the common ion effect, slowing down the polymerization. Further addition of LiCl above the threshold concentration should decrease the concentration of free $\text{Li}^+(\text{THF})_4$ cations, leading to enhanced $\text{PSt}-\text{Li}$ chain end dissociation, thus increasing the polymerization rate, in agreement with kinetic data reported in the literature.

Introduction

Lithium chloride is known to affect the anionic polymerization of methyl methacrylate (MMA) in ethereal solvents such as THF.¹ There is evidence that PMMA living chain ends form mixed aggregates with LiCl, predominantly existing in a dimeric form in THF solution,² of 1:1 and 2:1 compositions:¹



Extensive NMR studies of possible equilibria were published.³

The aggregation behavior in THF of methyl α -lithioisobutyrate (MIB-Li), simulating PMMA living chain ends, has been fully studied experimentally, using vapor phase osmometry⁴ and NMR methods.^{5,6} It has been well established^{4–6} that in THF solution there is an equilibrium between dimeric and tetrameric MIB-Li aggregates, the former prevailing at low and the latter at higher temperatures. Therefore, it has been reasonably suggested^{5,6} that the dimer is specifically solvated with THF molecules, unlike the tetramer, and is, therefore, energetically favorable but entropically unfavorable compared to the tetramer.

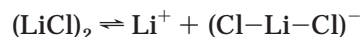
[†] Johannes Gutenberg Universität.

[‡] Permanent address: Institute of Macromolecular Compounds of the Russian Academy of Sciences, Bolshoi prospect 31, 199004 St. Petersburg, Russia.

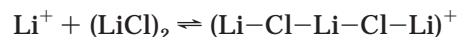
[§] New address: Macromolecular Chemistry II, University of Bayreuth, D-95440 Bayreuth, Germany. E-mail: axel.mueller@uni-bayreuth.de.

^{||} Katholieke Universiteit Leuven.

Experimental data on the effect of LiCl on the anionic polymerization of styrene (St) in tetrahydropyran (THP) solution show⁷ that addition of a 7-fold molar excess of LiCl retards the polymerization if LiCl concentration is low (about 10^{-4} mol/L for THP case) and accelerates it if LiCl concentration is high enough (about 10^{-2} mol/L in THP). These data were interpreted in terms of a prevailing ionogenic equilibrium into which LiCl is involved in an ethereal solvent, like THP or THF, depending on its concentration. Thus, if the LiCl concentration is low, Li^+ cations are mainly supplied into the solution via unimolecular dissociation of LiCl dimers:



suppressing the dissociation of living polymer chain ends, $\text{PSt}-\text{Li}$, by a common ion effect. As styrene polymerization in ethereal solvents is mainly propagated by free anions, PSt^- ,⁸ this results in slowing down the polymerization. On the other hand, at sufficiently high LiCl concentration, a bimolecular scavenging reaction of Li^+ by LiCl was proposed to dominate



thus promoting $\text{PSt}-\text{Li}$ dissociation and enhancing the polymerization rate.

The aim of the present paper is 2-fold: using the modern quantum-chemical density functional theory (DFT) approach, (1) to analyze the energetics of possible ionogenic reactions of LiCl itself in an ethereal solvent (THF) and (2) to study the solvent (THF) and the additive (LiCl) effects on the stability and structure of

models of PMMA–Li and PSt–Li living chain ends and their reactivities as anionic polymerization propagation centers.

It should be noted that the reactivity of PSt–Li living chains ends is considered to be determined by their ability to dissociate into free anions, PSt[−].⁸ Therefore, no attention to possible PSt–Li chain ends aggregation was paid. However, the reactivity of PMMA living chain ends is supposed to be dependent only on their aggregation state, because the equilibrium constant of their dissociation into free ions is very low.⁹ Earlier, some of us reported on ab initio Hartree–Fock calculations of MIB–Li aggregates.¹⁰ However, in that work, effects of the specific solvation by THF on the MIB–Li aggregation state were estimated only semiempirically.

Methods

All quantum-chemical calculations were carried out employing the TURBOMOLE package¹¹ of ab initio quantum chemical programs within the framework of the DFT approach.¹²

The geometries of all studied structures of the type (R–Li)_{*n*}(LiCl)_{*x*}(THF)_{*y*} were completely optimized. Active sites of MMA polymerization were simulated by α -lithiomethyl isobutyrate (MIB–Li) in both nonaggregated (*n* = 1) and aggregated (*n* = 2) states and those of St polymerization by 1-lithioethylbenzene (EB–Li) in a nonaggregated state (*n* = 1). Specific solvation by THF molecules was taken into account by adding the necessary amount of THF molecules so as to create a tetrahedral arrangement of electron donors (oxygen and/or chlorine atoms) around each of Li atoms.

For the DFT geometry optimizations, Becke's exchange potential¹³ and Perdew's correlation potential¹⁴ were used. This set of DFT potentials is hereafter referred to as BP86.

TURBOMOLE split valence plus polarization (SVP) basis sets¹⁵ of 6-31G* quality were employed. The details about contraction schemes and polarization function exponents for each element are described in the recently published paper.¹⁶ For all the structures optimized at the SVP/BP86 level, single-point energy calculations at the TZVP/B3–LYP level were performed using Karlsruhe TZVP basis sets, consisting of TZV basis sets¹⁷ of triple- ζ quality augmented with polarization functions for all atoms,¹⁶ and Becke's three-parameter functional¹⁸ with the correlation potential by Lee, Yang, and Parr.¹⁹ Calculating B3–LYP energies at the geometries optimized at a lower level of theory (including even semiempirical one) was recently justified by Abboto, Streitwieser, and Schleyer in their paper on the aggregation behavior of lithium enolate of acetaldehyde.²⁰

RI approximation,²¹ allowing one to approximate the Coulomb potential with high accuracy without calculations of four-centered two-electron integrals, was used at the SVP/BP86 level. The set of atom-centered auxiliary basis set (ABS) utilized by the RI approximation was the same as in ref 16.

In some cases, ¹³C NMR shifts, δ , on atoms of interest (mostly α -carbons of MIB–Li moieties) were calculated by the GIAO–SCF method²² implemented into the TURBOMOLE program²³ and compared with relevant experimental data. For the NMR calculations of all structures studied, Hartree–Fock molecular orbitals were calculated at the SVP/BP86-optimized geometries with the TZVP basis sets. Although no transition state structures were calculated in the present paper, we attempted to estimate the relative reactivity of MIB–Li aggregates as MMA propagation centers by comparing their chemical shifts for α -carbons. We believe that such a comparison is helpful because the chemical shifts are related to the electron density at α -carbons and, thus, to their reactivity with respect to the monomer.

For all LiCl-aggregated complexes with THF of the type (LiCl)_{*x*}(THF)_{*y*}, the values of a comparable stability parameter, the averaged energy per one LiCl molecule, $\bar{E}[(\text{LiCl})_x(\text{THF})_y]$, were calculated via eq 1, where $E[(\text{LiCl})_x(\text{THF})_y]$ and $E(\text{THF})$

$$\bar{E}[(\text{LiCl})_x(\text{THF})_y] = \frac{E[(\text{LiCl})_x(\text{THF})_y] - yE(\text{THF})}{x} \quad (1)$$

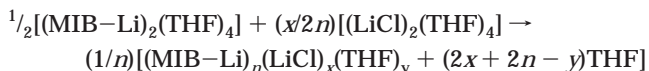
are the minimized total energy of the particular complex (LiCl)_{*x*}(THF)_{*y*} and THF molecule, respectively.

For all considered structures of the type (R–Li)_{*n*}(LiCl)_{*x*}(THF)_{*y*}, the values of the averaged energy per one active site, R–Li (either EB–Li or MIB–Li) fragment, $\bar{E}[(\text{R–Li})_n(\text{LiCl})_x(\text{THF})_y]$, were calculated as a comparable stability parameter

$$\bar{E}[(\text{R–Li})_n(\text{LiCl})_x(\text{THF})_y] = \frac{E[(\text{R–Li})_n(\text{LiCl})_x(\text{THF})_y] - x\bar{E}[(\text{LiCl})_2(\text{THF})_4] - yE(\text{THF})}{n} \quad (2)$$

where $E[(\text{R–Li})_n(\text{LiCl})_x(\text{THF})_y]$ is the minimized total energy of the particular complex (R–Li)_{*n*}(LiCl)_{*x*}(THF)_{*y*} and $\bar{E}[(\text{LiCl})_2(\text{THF})_4]$ is calculated via eq 1 for the (LiCl)₂(THF)₄ aggregate.

In addition to the specific solvation, taken into account by the explicit inclusion of THF molecules into the considered complexes, their nonspecific solvation by the solvent continuum may be of importance, especially for the structures with high degree of charge separation like solvent-separated ion pairs. To calculate nonspecific solvation energies, E_{NSS} , the SVP/BP86-optimized geometries of all structures were input into a specially modified semiempirical MOPAC 6.0 program.²⁴ In this program, a solute molecule is placed into a cavity of complex shape in the solvent continuum, formed by the intersecting van der Waals spheres surrounding the solute atoms. Then, the solvent polarization by the solute charge distribution and reverse polarization of the solute by the polarized solvent is calculated self-consistently.²⁴ The solvent polarity is characterized by the dielectric constant, ϵ . For these semiempirical calculations of E_{NSS} , MNDO parametrization²⁵ was used. Average values, \bar{E}_{NSS} , of nonspecific solvation energies were calculated analogously to eqs 1 and 2, using E_{NSS} values instead of total energy values (E). The relative thermodynamic stability of all studied compounds of the type (R–Li)_{*n*}(LiCl)_{*x*}(THF)_{*y*} in a polar solvent may be estimated by comparing their values of $\bar{E} + \bar{E}_{\text{NSS}}$. As may be derived from eqs 1 and 2, different stoichiometry of the complexes is taken into account in both \bar{E} and \bar{E}_{NSS} by subtracting (1) $(x/2)E[(\text{LiCl})_2(\text{THF})_4]$ and (2) $(y - 2x)E(\text{THF})$ from the total energy E of a given complex and dividing the residue by *n*. Therefore, the values of $\Delta(\bar{E} + \bar{E}_{\text{NSS}})$ presented in Table 4 are simply enthalpies of the following balanced reactions:



The results presented in this paper were obtained for $\epsilon = 12.13$, corresponding to the dielectric constant of THF at low temperature, about -70 °C, at which MMA anionic polymerization typically proceeds. It should be noted that (1) the anionic polymerization of St is usually being carried out at higher temperatures (between -20 and 20 °C) and (2) the ϵ value for THP is lower than that for THF. However, no qualitative changes in the obtained results were found when $\epsilon = 7.42$, which corresponds to the dielectric constant of THF at room temperature and is close to the ϵ value of THP at room temperature (5.71), was used.

Results and Discussion

1. LiCl Behavior in THF. Calculated DFT values of total energies, E , stability indices, \bar{E} , and MNDO-estimated nonspecific solvation energies, E_{NSS} , for all studied (LiCl)_{*x*}(THF)_{*y*} complexes are summarized in Table 1.

Table 1 presents the data concerning the energetics of gradual deaggregation of LiCl from dimeric to unimeric form upon increasing specific solvation by THF.

Table 1. DFT Results Related to LiCl Aggregation and Dissociation Behavior in THF

structure	E hartree		$\Delta\bar{E}$, kJ/mol	$\epsilon = 12.13$		$\Delta(\bar{E} + \bar{E}_{\text{nss}})$, kJ/mol	
		\bar{E} , hartree		\bar{E}_{nss} , kJ/mol	\bar{E}_{nss} , kJ/mol		
(LiCl) ₂ (THF) ₄ (Figure 1a)	<i>a</i>	-1864.636073	-467.776405	0	-63.7	-19.2	0
	<i>b</i>	-1865.205806	-467.833437	0			0
(LiCl) ₂ (THF) ₅ (Figure 1b)	<i>a</i>	-2096.911218	-467.778864	-6.4	-69.6	-18.9	-6.1
	<i>b</i>	-2097.590925	-467.83363	-0.5			-0.2
(LiCl)(THF) ₃	<i>a</i>	-1164.584553	-467.772459	10.4	-52.3	-33.3	-3.7
	<i>b</i>	-1164.982770	-467.828571	12.7			-1.4
(LiCl)(THF) ₄	<i>a</i>	-1396.859771	-467.776979	-1.5	-51.2	-25.7	-8.0
	<i>b</i>	-1397.366629	-467.827697	15.0			8.5
Cl ⁻	<i>a</i>	-460.129030			-293.2		
	<i>b</i>	-460.219244					
[Cl-Li(THF) ₂ -Cl] ⁻ (Figure 2a)	<i>a</i>	-1392.505056			-251.4		
	<i>b</i>	-1392.851720					
Li ⁺ (THF) ₄	<i>a</i>	-936.545041			-132.3		
	<i>b</i>	-937.003802					
[(THF) ₃ Li-Cl-Li(THF) ₃] ⁺	<i>a</i>	-1868.883567			-80.3		
	<i>b</i>	-1869.625363					
[(THF) ₃ Li-Cl-Li(THF) ₂ -Cl-Li(THF) ₃] ⁺ (Figure 2b)	<i>a</i>	-2801.208024			-139.0		
	<i>b</i>	-2802.233790					
THF	<i>a</i>	-232.270698			-6.4		
	<i>b</i>	-232.384733					

^a Calculated at the SVP/BP86//SVP/BP86 level. ^b Calculated at the TZVP/B3-LYP//SVP/BP86 level.

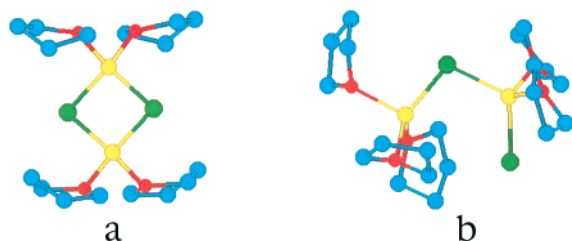


Figure 1. DFT-optimized geometries of the (LiCl)₂(THF)₄ complex (a) and the (LiCl)₂(THF)₅ zwitterionic complex (b). Hydrogens are omitted.

The reference structure is the (LiCl)₂(THF)₄ complex having *C*₂-symmetry (Figure 1a).

At the SVP/BP86 level, increasing the number of THF molecules per one LiCl molecule is, in general, favorable, as it leads to the decrease in the $\Delta(\bar{E} + \bar{E}_{\text{nss}})$ value. It is interesting to note that addition of one more THF molecule to the (LiCl)₂(THF)₄ complex breaks one of the Li-Cl bonds and leads to formation of an unsymmetric, zwitterionic complex of the composition (LiCl)₂(THF)₅ (Figure 1b) which is rather stable both in a vacuum ($\epsilon = 1$) and in polar medium ($\epsilon = 12.13$).

However, at the TZVP/B3-LYP level, the (LiCl)₂(THF)₅ and (LiCl)(THF)₃ complexes are almost as stable as the reference (LiCl)₂(THF)₄ complex: $\Delta(\bar{E} + \bar{E}_{\text{nss}}) = -0.06$ and -1.3 kJ/mol, respectively. This result agrees with the experimentally found dominating dimeric form of LiCl in THF solution,² because such a small energy gain for the (LiCl)(THF)₃ complex with respect to the (LiCl)₂(THF)₄ complex is, undoubtedly, less important than the entropic losses due to additional specific solvation.

Table 2 presents the DFT enthalpies of dissociation reactions of the (LiCl)₂(THF)₄ complex calculated per LiCl molecule as differences in the \bar{E} values between the products (pairs of free ions) and reagent ((LiCl)₂(THF)₄ complex of contact ion pair type) of these reactions. As seen from the data of Table 2, the dissociation enthalpies are systematically lower at the TZVP/B3-LYP level than at the SVP/BP86 level. The most energetically favorable dissociation of (LiCl)₂(THF)₄ is that into a triple anion [Cl-Li(THF)₂-Cl]⁻

(Figure 2a) and a quintuple cation [(THF)₃Li-Cl-Li(THF)₂-Cl-Li(THF)₃]⁺ (Figure 2b). At the higher level of theory, this dissociation reaction is almost thermo-neutral if nonspecific solvation is taken into account.

According to NMR data for allylic lithium compounds,²⁶⁻²⁸ the Li atom in triple anions of the (allyl-Li-allyl)⁻ kind is not solvated. Conductivity studies of THF solution of LiCl also showed that the data are better reproduced theoretically if one assumes that in a triple anion (Cl-Li-Cl)⁻ the central Li atom is not solvated.²⁹ The reason for this is, probably, of entropic nature, as our DFT data show that THF solvation of the Li atom within the triple anion is energetically favorable.

In Table 3 calculated enthalpies of scavenging reactions of Li⁺(THF)₄ by (LiCl)₂(THF)₄ are given. The results are qualitatively similar at both levels of theory. It is seen that the formation of a quintuple cation [(THF)₃Li-Cl-Li(THF)₂-Cl-Li(THF)₃]⁺, as a result of the scavenging, is thermodynamically favorable (the enthalpy is negative) both in a vacuum and in the polar solvent. The formation of triple cation, [(THF)₃Li-Cl-Li(THF)₃]⁺, being most preferable in a vacuum, is thermodynamically unfavorable in the polar medium.

2. Aggregation Behavior of MIB-Li, as a Model of the PMMA Living Chain End, in THF Solution.

Table 4 contains calculated DFT values of total energies, E , stability indices, \bar{E} , and MNDO-estimated nonspecific solvation energy, E_{nss} , values for all (MIB-Li)_{*n*}(LiCl)_{*x*}(THF)_{*y*} complexes. The reference structure is the dimeric complex (MIB-Li)₂(THF)₄ of *C*₂-symmetry (Figure 3a). It is seen from Table 4 that MIB-Li may form a LiCl-free zwitterionic complex (MIB-Li)₂(THF)₅ (Figure 3b), replacing the enolate oxygen atom at the coordination site of one of the Li atoms with a THF molecule, for reasonably low energy costs ($\Delta(\bar{E} + \bar{E}_{\text{nss}}) = 4.7$ and 9.7 kJ/mol at the SVP/BP86 and TZVP/B3-LYP levels, respectively) and with higher reactivity. The difference of calculated chemical shifts of the α -carbon atom, $\Delta\delta = -3.53$ ppm, indicates a higher electron density at this atom in (MIB-Li)₂(THF)₅ compared to that in (MIB-Li)₂(THF)₄. Further addition of THF leads to the formation of a unimeric complex of the composition (MIB-

Table 2. DFT-Calculated Enthalpies, ΔH , of $(\text{LiCl})_2(\text{THF})_4$ Dissociation Reactions (kJ/mol per LiCl Molecule)

dissociation reaction	ϵ	ΔH , kJ/mol	
$\frac{1}{2}[(\text{LiCl})_2(\text{THF})_4] + 2\text{THF} \rightarrow \text{Li}^+(\text{THF})_4 + \text{Cl}^-$	1	a	485.5
	12.13	b	391.7
$\frac{1}{2}[(\text{LiCl})_2(\text{THF})_4] + \text{THF} \rightarrow \frac{1}{2}[(\text{THF})_3\text{Li}-\text{Cl}-\text{Li}(\text{THF})_3]^+ + \frac{1}{2}\text{Cl}^-$	1	a	104.5
	12.13	b	10.7
$\frac{1}{2}[(\text{LiCl})_2(\text{THF})_4] + \text{THF} \rightarrow \frac{1}{2}[\text{Li}^+(\text{THF})_4] + \frac{1}{2}[\text{Cl}-\text{Li}(\text{THF})_2-\text{Cl}]^-$	1	a	215.6
	12.13	b	171.4
$\frac{1}{2}[(\text{LiCl})_2(\text{THF})_4] + \frac{2}{3}\text{THF} \rightarrow \frac{1}{3}[(\text{THF})_3\text{Li}-\text{Cl}-\text{Li}(\text{THF})_2-\text{Cl}-\text{Li}(\text{THF})_3]^+ + \frac{1}{3}\text{Cl}^-$	1	a	67.1
	12.13	b	22.9
$\frac{1}{2}[(\text{LiCl})_2(\text{THF})_4] + \frac{2}{3}\text{THF} \rightarrow \frac{1}{3}[(\text{THF})_3\text{Li}-\text{Cl}-\text{Li}(\text{THF})_3]^+ + \frac{1}{3}[\text{Cl}-\text{Li}(\text{THF})_2-\text{Cl}]^-$	1	a	137.9
	12.13	b	109.4
$\frac{1}{2}[(\text{LiCl})_2(\text{THF})_4] + \frac{1}{2}\text{THF} \rightarrow \frac{1}{4}[(\text{THF})_3\text{Li}-\text{Cl}-\text{Li}(\text{THF})_2-\text{Cl}-\text{Li}(\text{THF})_3]^+ + \frac{1}{4}[\text{Cl}-\text{Li}(\text{THF})_2-\text{Cl}]^-$	1	a	30.0
	12.13	b	1.5
$\frac{1}{2}[(\text{LiCl})_2(\text{THF})_4] + \text{THF} \rightarrow \frac{1}{2}[\text{Li}^+(\text{THF})_4] + \frac{1}{2}[\text{Cl}-\text{Li}(\text{THF})_2-\text{Cl}]^-$	1	a	166.4
	12.13	b	157.0
$\frac{1}{2}[(\text{LiCl})_2(\text{THF})_4] + \frac{2}{3}\text{THF} \rightarrow \frac{1}{3}[(\text{THF})_3\text{Li}-\text{Cl}-\text{Li}(\text{THF})_3]^+ + \frac{1}{3}[\text{Cl}-\text{Li}(\text{THF})_2-\text{Cl}]^-$	1	a	12.8
	12.13	b	3.4
$\frac{1}{2}[(\text{LiCl})_2(\text{THF})_4] + \frac{1}{2}\text{THF} \rightarrow \frac{1}{4}[(\text{THF})_3\text{Li}-\text{Cl}-\text{Li}(\text{THF})_2-\text{Cl}-\text{Li}(\text{THF})_3]^+ + \frac{1}{4}[\text{Cl}-\text{Li}(\text{THF})_2-\text{Cl}]^-$	1	a	92.8
	12.13	b	88.4
$\frac{1}{2}[(\text{LiCl})_2(\text{THF})_4] + \frac{1}{2}\text{THF} \rightarrow \frac{1}{4}[(\text{THF})_3\text{Li}-\text{Cl}-\text{Li}(\text{THF})_2-\text{Cl}-\text{Li}(\text{THF})_3]^+ + \frac{1}{4}[\text{Cl}-\text{Li}(\text{THF})_2-\text{Cl}]^-$	1	a	18.3
	12.13	b	13.9
$\frac{1}{2}[(\text{LiCl})_2(\text{THF})_4] + \frac{1}{2}\text{THF} \rightarrow \frac{1}{4}[(\text{THF})_3\text{Li}-\text{Cl}-\text{Li}(\text{THF})_2-\text{Cl}-\text{Li}(\text{THF})_3]^+ + \frac{1}{4}[\text{Cl}-\text{Li}(\text{THF})_2-\text{Cl}]^-$	1	a	65.2
	12.13	b	62.7
		a	2.6
		b	0.1

^a Calculated at the SVP/BP86//SVP/BP86 level. ^b Calculated at the TZVP/B3-LYP//SVP/BP86 level.

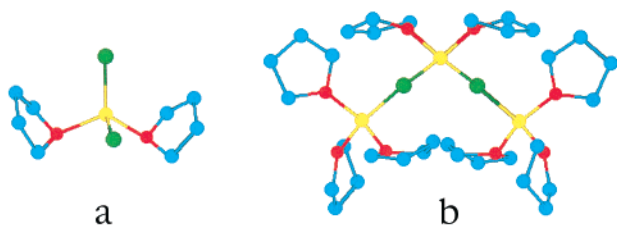


Figure 2. DFT-optimized geometries of the triple anion $[\text{Cl}-\text{Li}(\text{THF})_2-\text{Cl}]^-$ (a) and quintuple cation $[(\text{THF})_3\text{Li}-\text{Cl}-\text{Li}(\text{THF})_3]^+$ (b). Hydrogens are omitted.

$\text{Li}(\text{THF})_3$ (Figure 3c), the latter being even more stable ($\Delta(\bar{E} + \bar{E}_{\text{nss}}) = 3.0$ and 5.8 kJ/mol at the SVP/BP86 and TZVP/B3-LYP levels, respectively) and having considerably higher electron density at the α -carbon atom ($\Delta\delta = -14.08$ ppm) than the complex $(\text{MIB}-\text{Li})_2(\text{THF})_5$. Complexes with such strongly upfield shifted ^{13}C NMR α -carbon peaks were found for MIB-Li in THF in the presence of cryptands and was shown to be extremely reactive in anionic polymerization of MMA.³⁰

3. Effect of LiCl on the Aggregation Behavior of MIB-Li in THF Solution. As seen from $\Delta(\bar{E} + \bar{E}_{\text{nss}})$ values in Table 4, the most stable and the only energetically favorable complex among the mixed complexes of MIB-Li with LiCl is the 1:1 complex (Figure 4a). Other mixed aggregates of the compositions 1:1 (Figures 4b), 1:2 (Figure 5a), and 2:1 (Figure 5b) are predicted to be considerably less stable at the TZVP/B3-LYP level than at the SVP/BP86 level.

Comparing their calculated ^{13}C NMR α -carbon shifts to that of the LiCl-free $(\text{MIB}-\text{Li})_2(\text{THF})_4$ complex (Figure 3a), one can see that square-like complex $(\text{MIB}-\text{Li})(\text{LiCl})(\text{THF})_4$ (Figure 4a) should be less reactive ($\Delta\delta = 2.54$ ppm, i.e., electron density at α -carbon decreases compared to that for the $(\text{MIB}-\text{Li})_2(\text{THF})_4$ complex). The experimental value of $\Delta\delta = 1$ ppm found for the equimolar complex between LiCl and MIB-Li³¹ is in a very good agreement with this result.

The zwitterionic complex $(\text{MIB}-\text{Li})(\text{LiCl})(\text{THF})_5$ (Figure 4b) should be more reactive than the $(\text{MIB}-\text{Li})_2(\text{THF})_4$ complex ($\Delta\delta = -3.72$ ppm). As it is not of

formidably high energy (even at the TZVP/B3-LYP level, it is ca. $8 kT$ at -70° , compared to the $(\text{MIB}-\text{Li})_2(\text{THF})_4$ complex), these results can explain experimental data¹ about an increase in the MMA polymerization rate with increase in molar ratio, R , of LiCl added with respect to the living chain end concentration, provided $R < 1$.

The calculated ^{13}C NMR α -carbon signal for the $(\text{MIB}-\text{Li})(\text{LiCl})_2(\text{THF})_6$ 1:2 complex (Figure 5a) is by ca. 2.3 ppm downfield shifted compared to that of the $(\text{MIB}-\text{Li})(\text{LiCl})(\text{THF})_4$ 1:1 complex (Figure 4a), in agreement with slowing down MMA polymerization upon further LiCl addition ($1 < R \leq 10$).¹ Downfield shifts of the α -carbon ^{13}C NMR signal of di-*tert*-butyl 2-lithio-2,4,4-trimethylglutarate were also found upon its mixing with LiCl.³ MNDO calculations³ indicated the possible formation of both 2:2 and 2:4 mixed complexes of α -lithio ester enolates with LiCl, which may be considered as dimerized 1:1 (Figure 4a) and 1:2 (Figure 5a) complexes studied here. The lack of accounting for solvation effects, both specific and nonspecific, should be noted with regard to these MNDO data. In particular, it could be the reason for the considerably higher MNDO-predicted stability of the 1:2 complex between ester enolate and LiCl compared to that of 1:1 complex (by > 100 kJ/mol). This is obviously not the case for the DFT data obtained in the present work: the 1:2 complex ($\Delta(\bar{E} + \bar{E}_{\text{nss}}) = 7.8$ and 17.4 kJ/mol at the SVP/BP86 and TZVP/B3-LYP levels, respectively) is by more than 16 kJ/mol less stable than the 1:1 complex ($\Delta(\bar{E} + \bar{E}_{\text{nss}}) = -9.4$ and -4.3 kJ/mol at the SVP/BP86 and TZVP/B3-LYP levels, respectively). Moreover, the 2:2 cubelike mixed complex $(\text{MIB}-\text{Li})_2(\text{LiCl})_2(\text{THF})_4$ (Figure 5c) has a very high relative energy (more than 25 kJ/mol) at both theory levels and a rather low electron density at the α -carbon atoms ($\Delta\delta = 6.93$ ppm). The experimentally found presence of associated PMMA living chains at very high LiCl concentrations³² may be due to formation of 2:1 complexes (Figure 5b).

4. Effect of LiCl on Ionogenic Reactions of PSt-Li Active Sites in THF Solution. 1-Lithioethylben-

Table 3. Calculated Enthalpies of Reactions of $\text{Li}^+(\text{THF})_4$ with $(\text{LiCl})_2(\text{THF})_4$

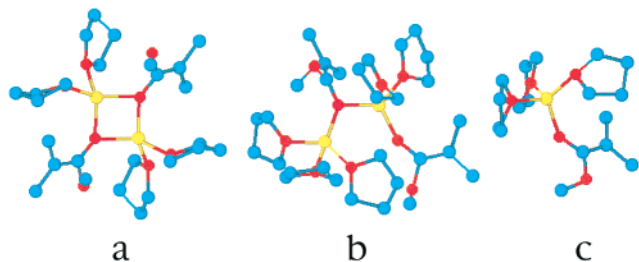
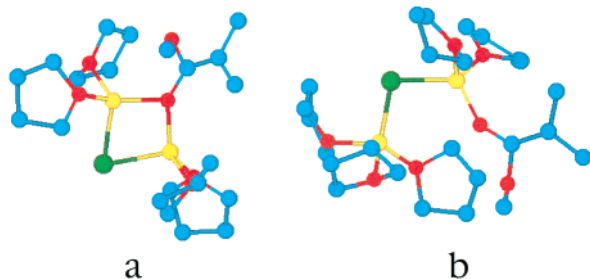
reaction		ΔH , kJ/mol	
		$\epsilon = 1$	$\epsilon = 12.13$
$\text{Li}^+(\text{THF})_4 + \frac{1}{2}(\text{LiCl})_2(\text{THF})_4 \rightarrow [(\text{THF})_3\text{Li}-\text{Cl}-\text{Li}(\text{THF})_3]^+$	<i>a</i>	-53.8	30.1
	<i>b</i>	-48.9	35.0
$\text{Li}^+(\text{THF})_4 + (\text{LiCl})_2(\text{THF})_4 \rightarrow [(\text{THF})_3\text{Li}-\text{Cl}-\text{Li}(\text{THF})_2-\text{Cl}-\text{Li}(\text{THF})_3]^+$	<i>a</i>	-70.6	-13.6
	<i>b</i>	-63.4	-6.4

^a Calculated at the SVP/BP86//SVP/BP86 level. ^b Calculated at the TZVP/B3-LYP//SVP/BP86 level.

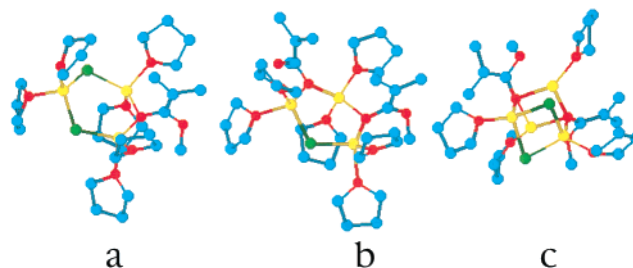
Table 4. DFT Results for the Most Stable MIB-Li Aggregates in THF in the Presence of LiCl (with Hartree-Fock ^{13}C NMR Shifts, δ , at α -Carbon Atoms Calculated at DFT-Optimized Geometries)

structure	<i>E</i> hartree	\bar{E} , hartree	$\Delta\bar{E}$, kJ/mol	$\epsilon = 12.13$		$\Delta(\bar{E} + \bar{E}_{\text{nss}})$, kJ/mol	δ , ppm	$\Delta\delta$, ppm	
				E_{nss} , kJ/mol	\bar{E}_{nss} , kJ/mol				
(MIB-Li) ₂ (THF) ₄ (Figure 3a)	<i>a</i>	-1636.591870	-353.754539	0	-44.2	-9.4	0	74.16	0
	<i>b</i>	-1637.405176	-353.933122	0			0		
(MIB-Li) ₂ (THF) ₅ (Figure 3b)	<i>a</i>	-1868.858173	-353.752364	5.7	-52.6	-10.4	4.7	70.63; 71.58	-3.53; -2.58
	<i>b</i>	-1869.781777	-353.929056	10.7			9.7		
(MIB-Li)(THF) ₃ (Figure 3c)	<i>a</i>	-1050.559138	-353.747044	19.6	-45.1	-26.0	3.0	60.08	-14.08
	<i>b</i>	-1051.078760	-353.924561	22.4			5.8		
(MIB-Li) ₄ (ref 13)	<i>a</i>	-1414.943231	-353.735808	49.1				83.40	9.24
	<i>b</i>	-1415.673969	-353.918492	38.4					
(MIB-Li) ₆ (ref 13)	<i>a</i>	-2122.447428	-353.741238	34.9				85.40	11.24
	<i>b</i>	-2123.541494	-353.923582	25.0					
(MIB-Li)(LiCl)(THF) ₄ (Figure 4a)	<i>a</i>	-1750.617888	-353.758456	-10.3	-53.1	-8.6	-9.5	76.70	2.54
	<i>b</i>	-1751.307459	-353.935090	-5.1			-4.3		
(MIB-Li)(LiCl)(THF) ₅ (Figure 4b)	<i>a</i>	-1982.882997	-353.752867	4.4	-62.2	-11.2	2.6	70.44	-3.72
	<i>b</i>	-1983.683986	-353.926884	16.3			14.5		
(MIB-Li)(LiCl) ₂ (THF) ₆ (Figure 5a)	<i>a</i>	-2682.934974	-353.757505	-7.8	-70.3	6.1	7.7	79.01	4.85
	<i>b</i>	-2683.907681	-353.932409	1.9			17.4		
(MIB-Li) ₂ (LiCl)(THF) ₆ (Figure 5b)	<i>a</i>	-2568.912581	-353.755876	-3.5	-57.7	-0.2	5.7	76.50; 80.46	2.34; 6.30
	<i>b</i>	-2570.005413	-353.931789	3.5			12.7		
(MIB-Li) ₂ (LiCl) ₂ (THF) ₄ (Figure 5c)	<i>a</i>	-2572.129046	-353.746487	21.1	-60.4	1.7	32.2	81.09	6.93
	<i>b</i>	-2573.057316	-353.925755	19.3			30.4		

^a Calculated at the SVP/BP86//SVP/BP86 level. ^b Calculated at the TZVP/B3-LYP//SVP/BP86 level.

**Figure 3.** DFT-optimized geometries of (MIB-Li)₂(THF)₄ (a), (MIB-Li)₂(THF)₅ (b), and (MIB-Li)(THF)₃ (c). Hydrogens are omitted.**Figure 4.** DFT-optimized geometries of (MIB-Li)(LiCl)(THF)₄ (a) and (MIB-Li)(LiCl)(THF)₅ (b). Hydrogens are omitted.

zene (EB-Li) was used as a model compound for PSt-Li chain ends. Calculated DFT values of total energies, E , stability indices, \bar{E} , and MNDO-estimated nonspecific solvation energy, E_{nss} , values for all studied (EB-Li)-(LiCl)_x(THF)_y complexes are collected in Table 5. It is seen that the formation of the THF-separated ion pair, EB⁻/[Li(THF)₄]⁺ (Figure 6a), is thermodynamically

**Figure 5.** DFT-optimized geometries of (MIB-Li)(LiCl)₂(THF)₆ (a), (MIB-Li)₂(LiCl)(THF)₆ (b), and (MIB-Li)₂(LiCl)₂(THF)₄ (c). Hydrogens are omitted.

favorable in THF solution. However, from the experimental point of view, such ion pairs are only indirectly observed for PSt-Li in THF through kinetic measurements.^{33,34} According to the calculated data presented in Table 6, their dissociation is endothermic (for $\epsilon = 12.13$, $\Delta H = 31.5$ and 15.7 kJ/mol at the SVP/BP86 and TZVP/B3-LYP levels, respectively). It means that gain in the nonspecific solvation energy due to the dissociation is small compared to the Coulomb attraction energy within the ion pair. Therefore; the ion pair dissociation into free ions should lead to no considerable solvent confinement, and can be entropically favorable.

Experimentally, PSt-Li chain ends were shown to be solvated with only two THF molecules,^{34,35} and their overall dissociation into free ions in THF was found to be slightly exothermic.³⁶ Our calculations confirm the exothermicity of the dissociation of the (EB-Li)(THF)₂ complex (Table 6). However, the DFT data presented in Table 5 show that the (EB-Li)(THF)₂ complex is enthalpically less stable than (EB-Li)(THF)₃, at both

Table 5. DFT Results Related to the Effect of LiCl on Ionogenic Reactions of PSt–Li Active Sites in THF Solution

structure	<i>E</i> hartree	\bar{E} , hartree	$\Delta\bar{E}$, kJ/mol	$\epsilon = 12.13$			
				E_{nss} , kJ/mol	\bar{E}_{nss} , kJ/mol	$\Delta(\bar{E} + \bar{E}_{\text{nss}})$, kJ/mol	
C ₆ H ₅ –CH(CH ₃)–Li(THF) ₃	<i>a</i>	–1014.410443	–317.598349	0	–47.7	–28.6	0
	<i>b</i>	–1014.874294	–317.720095	0			0
C ₆ H ₅ –CH(CH ₃)–Li(THF) ₂	<i>a</i>	–782.129776	–317.588380	26.2	–37.0	–24.3	30.5
	<i>b</i>	–782.482090	–317.712624	19.6			23.9
C ₆ H ₅ –CH(CH ₃) [–] /Li ⁺ (THF) ₄ solvent-separated ion pair (Figure 6a)	<i>a</i>	–1246.674177	–317.591385	18.3	–88.2	–62.8	–15.9
	<i>b</i>	–1247.249611	–317.710679	24.7			–9.5
C ₆ H ₅ –CH(CH ₃) [–]	<i>a</i>	–310.021933			–205.6		
	<i>b</i>	–310.144613					
C ₆ H ₅ –CH(CH ₃)–Li(THF) ₂ –Cl [–] (Figure 6b)	<i>a</i>	–1242.345407			–219.7		
	<i>b</i>	–1242.753411					

^a Calculated at the SVP/B–P//SVP/B–P level. ^b Calculated at the TZVP/B3–LYP//SVP/B–P level.

Table 6. Calculated Enthalpies of Model PSt–Li Active Site Dissociation Reactions

reaction	ΔH , kJ/mol		
	$\epsilon = 1$	$\epsilon = 12.13$	
C ₆ H ₅ –CH(CH ₃)–Li(THF) ₃ + THF → (THF) ₄ Li ⁺ + C ₆ H ₅ –CH(CH ₃) [–]	<i>a</i>	299.5	15.6
	<i>b</i>	290.2	6.3
C ₆ H ₅ –CH(CH ₃)–Li(THF) ₂ + 2THF → (THF) ₄ Li ⁺ + C ₆ H ₅ –CH(CH ₃) [–]	<i>a</i>	273.3	–14.9
	<i>b</i>	270.5	–17.7
C ₆ H ₅ –CH(CH ₃)–Li(THF) ₃ + 1/2(LiCl) ₂ (THF) ₄ + THF → (THF) ₄ Li ⁺ + C ₆ H ₅ –CH(CH ₃)–Li(THF) ₂ –Cl [–]	<i>a</i>	285.2	19.1
	<i>b</i>	274.7	8.6
C ₆ H ₅ –CH(CH ₃)–Li(THF) ₂ + 1/2(LiCl) ₂ (THF) ₄ + 2THF → (THF) ₄ Li ⁺ + C ₆ H ₅ –CH(CH ₃)–Li(THF) ₂ –Cl [–]	<i>a</i>	259.0	–11.4
	<i>b</i>	255.1	–15.3
C ₆ H ₅ –CH(CH ₃) [–] /Li ⁺ (THF) ₄ → C ₆ H ₅ –CH(CH ₃) [–] + Li ⁺ (THF) ₄	<i>a</i>	281.2	31.5
	<i>b</i>	265.4	15.7

^a Calculated at the SVP/B–P//SVP/B–P level. ^b Calculated at the TZVP/B3–LYP//SVP/B–P level.

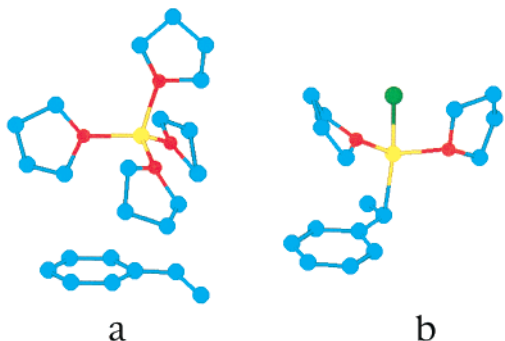


Figure 6. DFT-optimized geometries of THF-separated ion pair (EB[–])Li⁺(THF)₄ (a) and anion (EB[–])(LiCl)(THF)₂ (b). Hydrogens are omitted.

SVP/BP86 and TZVP/B3–LYP levels of theory. Therefore, experimental evidence³⁶ indicating the (EB–Li)–(THF)₂ complex to be the predominant species is probably due to its entropic preference with respect to the (EB–Li)(THF)₃ complex.

The data of Table 6 show that the dissociation of (EB–Li)(THF)_{*y*} complexes (*y* = 2, 3) is not promoted by EB[–] complexation with the LiCl molecule (the geometry of this complex is shown in Figure 6b). This result was obtained at both levels of theory. Thus, LiCl should affect styrene anionic polymerization rate only through the change of the concentration of PSt[–] polymer propagation active centers due to Li⁺(THF)₄ scavenging from PSt–Li or suppression of the dissociation of PSt–Li into PSt[–] anion and Li⁺(THF)₄ cation.

Acknowledgment. This work was supported by INTAS (Grant INTAS-RFBR 95-165). A.V.Y. expresses his gratitude to the Deutsche Forschungsgemeinschaft for financial support.

References and Notes

- (1) Kunkel, D.; Müller, A. H. E.; Janata, M.; Lochmann, L. *Makromol. Chem., Macromol. Symp.* **1992**, *60*, 315.
- (2) Wong, M. K.; Popov, A. I. *J. Inorg. Nucl. Chem.* **1972**, *34*, 3615.
- (3) (a) Wang, J. S.; Jérôme, R.; Warin, R.; Teyssié, Ph. *Macromolecules* **1993**, *26*, 1402. (b) Zune, C.; Dubois, P.; Jérôme, R.; Kříž, J.; Dybal, J.; Lochmann, L.; Janata, M.; Vlcek, P.; Werkhoven, T. M.; Lugtenburg, J. *Macromolecules* **1998**, *31*, 2744.
- (4) Halaska, V.; Lochmann, L. *Collect. Czech. Chem. Commun.* **1973**, *38*, 1780.
- (5) Wang, J. S.; Jérôme, R.; Warin, R.; Teyssié, Ph. *Macromolecules* **1993**, *26*, 1402.
- (6) Kříž, J.; Dybal, J.; Vlcek, P.; Janata, M. *Macromol. Chem. Phys.* **1994**, *195*, 3039.
- (7) Van Beylen, M.; Van Lierde, P.; Zimm, B. H.; Szwarc, M. *Macromol. Rapid Commun.* **1997**, *18*, 113.
- (8) Szwarc, M. *Carbanions, living polymers, and electron-transfer processes*, John Wiley & Sons: New York, London, 1968; p 415.
- (9) Dotcheva, D.; Tsvetanov, Ch. B.; Lochmann, L. *J. Polym. Sci., Polym. Chem. Ed.* **1987**, *25*, 3005.
- (10) Weiss, H.; Yakimansky, A. V.; Müller, A. H. E. *J. Am. Chem. Soc.* **1996**, *118*, 8897.
- (11) Ahlrichs, R.; Bär, M.; Häser, M.; Horn, H.; Kölmel, C. *Chem. Phys. Lett.* **1989**, *162*, 165.
- (12) Parr, R. G.; Yang, W. *Density-functional theory of atoms and molecules*; Oxford University Press: Oxford, England, 1989.
- (13) Becke, A. D. *Phys. Rev. A* **1988**, *38*, 3098.
- (14) Perdew, J. P. *Phys. Rev. B* **1986**, *33*, 8822.
- (15) Schäfer, A.; Horn, H.; Ahlrichs, R. *J. Chem. Phys.* **1992**, *97*, 2571.
- (16) Yakimansky, A. V.; Müller, A. H. E. *Macromolecules* **1999**, *32*, 1731.
- (17) Schäfer, A.; Huber, C.; Ahlrichs, R. *J. Chem. Phys.* **1994**, *100*, 5829.
- (18) Becke, A. D. *J. Chem. Phys.* **1993**, *98*, 5648.
- (19) Lee, C.; Yang, W.; Parr, R. G. *Phys. Rev. B* **1988**, *37*, 785.
- (20) Abbotto, A.; Streitwieser, A.; Schleyer, P. v. R. *J. Am. Chem. Soc.* **1997**, *119*, 11255.
- (21) Eichkorn, K.; Treuter, O.; Öhm, H.; Häser, M.; Ahlrichs, R. *Chem. Phys. Lett.* **1995**, *242*, 652.
- (22) Ditchfield, R. *Mol. Phys.* **1974**, *27*, 789.

- (23) Häser, M.; Ahlrichs, R.; Baron, H. P.; Weis, P.; Horn, H. *Theor. Chim. Acta* **1992**, *83*, 455.
- (24) Chudinov, G. E.; Napolov, D. V.; Basilevsky, M. V. *Chem. Phys.* **1992**, *160*, 41.
- (25) Dewar, M. J. S.; Thiel, W. *J. Am. Chem. Soc.* **1977**, *99*, 4899.
- (26) Paquette, L. A.; Bauer, W.; Sivik, M. R.; Bühl, M.; Feigel, M.; Schleyer, P. v. R. *J. Am. Chem. Soc.* **1990**, *112*, 8767.
- (27) Ronsberg, F. E.; Gilchrist, J. A.; Collum, D. B. *J. Am. Chem. Soc.* **1991**, *113*, 5751.
- (28) Jackman, L. M.; Scarmoutzos, L. M.; Porter, W. *J. Am. Chem. Soc.* **1987**, *109*, 5624.
- (29) (a) Verheyden, H.; Van Lierde, P.; Szwarc, M.; Litvinenko, G.; Van Beylen, M. *Proceedings, IP'99 IUPAC International Symposium on Ionic Polymerization 1999*, Kyoto, Japan, 1999; p 113. (b) Verheyden, H.; Van Lierde, P.; Litvinenko, G.; Szwarc, M.; Van Beylen, M. To be submitted to *Macromolecules*.
- (30) Wang, J. S.; Jérôme, R.; Warin, R.; Zhang, H.; Teyssié, Ph. *Macromolecules* **1994**, *27*, 3376.
- (31) Wang, J. S.; Warin, R.; Jérôme, R.; Teyssié, Ph. *Macromolecules* **1993**, *26*, 6776.
- (32) Kunkel, D. Dissertation, University of Mainz **1992**.
- (33) Peeters, S.; Gils, F.; Van Beylen, M. *Proceedings, 28th IUPAC International Symposium on Macromolecules*, Amherst, MA, 1982; p 104.
- (34) Bastiaens, J.; Huyskens, P.; Van Beylen, M. *Macromol. Symp.* **1998**, *132*, 165.
- (35) Smid, J. In *Structure and Mechanism of Vinyl Polymerization*, Tsuruta, T., O'Driscoll, K. F., Eds.; Marcel Dekker: New York, 1969; p 345.
- (36) Szwarc, M.; Van Beylen, M. *Ionic Polymerization and Living Polymers*; Chapman & Hall, New York, London, 1993; p 105.

MA9921549